

Safety Limits for Pre-Tension of Membrane Roofs on Closed Structure in Air Flow

WeiJu Song^{1,2,3*}, Heyuan Yang^{1,3}, Heding Yu²

¹School of Civil Engineering, Tianjin University, Tianjin, China

²Huaheng Construction Group, Ningbo, China

³School of Civil Engineering, Hebei University of Engineering, Handan, China

Email: *nimrodsong@126.com

How to cite this paper: Song, W.J., Yang, H.Y. and Yu, H.D. (2024) Safety Limits for Pre-Tension of Membrane Roofs on Closed Structure in Air Flow. *Applied Mathematics*, 15, 818-827.

<https://doi.org/10.4236/am.2024.1511045>

Received: November 1, 2024

Accepted: November 23, 2024

Published: November 26, 2024

Copyright © 2024 by author(s) and Scientific Research Publishing Inc.

This work is licensed under the Creative Commons Attribution International License (CC BY 4.0).

<http://creativecommons.org/licenses/by/4.0/>



Open Access

Abstract

The stiffness required for the normal operation of membrane roof comes from the application of pre-tension. When the pre-tension is too small, it is easy to cause instability under the action of wind load, which leads to excessive deformation of the roof and local or overall damage. In order to ensure that the membrane roof is always in normal use state in the airflow field, this paper takes the membrane pretension as the control parameter to study the value of safety pretension of closed membrane roof. According to the theory of large deflection of membrane and Galerkin method, the nonlinear vibration differential equation of membrane roof under static wind is established, and the critical state of safe working of membrane roof is determined by judging the stability of the solution of the equation, and the expression of critical wind speed is obtained. By establishing the inequality relationship between local design wind speed and critical wind speed, the safety pretension limit of membrane roof under specific site can be obtained. The research shows that the safety pretension limits of closed membrane roofs are different in different areas under different design return periods. In addition, the value of safety pretension is related to the film geometry.

Keywords

Membrane Roof, Pre-Tension, Aerodynamic Stability, Critical Wind Speed

1. Introduction

Membrane materials are usually used as enclosure materials (such as membrane roofs) or structural materials (such as inflatable membrane structures) in stadiums, architectural sketches and other buildings. These widely used membranes

have small dead weight and low stiffness, which leads to extremely easy vibration under wind load. If the initial pre-tension of the membrane is too small, it may lead to instability of the membrane roof, and the membrane will be torn and destroyed due to excessive vibration amplitude. In history, there are many engineering cases of membrane roof damage. Atlanta Georgia Dome, Japan Xiongdong Park membrane structure roof, Guangzhou Yihe Mountain Villa membrane structure, Jiaxing Pinghu Gymnasium membrane roof, etc. all suffer from instability and damage when the wind speed is lower than the design, which shows that the value of membrane pre-tension according to the current technical regulations of membrane structure cannot completely guarantee the safe use of membrane structure.

The stiffness of roofing membrane mainly comes from the initial tensile force applied to the membrane. Studies by Shen Shizhao, Wu Yue and other scholars have shown that [1]: When the flexible membrane structure is in a relaxed state, that is, when the pre-tension is insufficient, instability will occur, leading to the destruction of the membrane structure. For the study of instability and failure of membrane structure, in 2011, Zheng Zhoulian *et al.* determined the critical state of instability of small sag flat membrane structure and saddle membrane structure under wind load, and proved that the critical wind speed of instability is related to the initial pretension of membrane material [2] [3]; In 2015, Chen Zhaoqing *et al.* conducted aeroelastic model wind tunnel test of unidirectional tension membrane roof and discussed its instability mechanism [4]. In 2017, Liu *et al.* studied the stability of tensile membrane structure under wind load by Galerkin method, and obtained the main control factors to improve the stability of membrane structure [5]. In addition, many scholars have studied the wind-induced vibration response of membrane structures, but they have not quantitatively given the specific limits of pretension to prevent wind-induced damage [6]-[10]. The purpose of this paper is to determine the safe pretension limit of membrane roof in air flow field so as to avoid the occurrence of instability.

In this paper, the dynamic control equation of closed membrane roof under wind load is established, and the improved multi-scale method is used to solve it analytically. The closed expression of critical wind speed of instability is obtained by judging the criterion of critical condition of instability, and the inequality between site design wind speed and critical wind speed is established, and the safety pretension limit of closed membrane roof is obtained to prevent instability under specific wind field, which provides theoretical basis for determining the pretension in membrane structure design.

2. Derivation of Critical Wind Speed Expression for Instability of Membrane Roof

With the vibration of membrane roof, the transverse amplitude of membrane is relatively large, which is in the same order of magnitude as the thickness of membrane, showing a strong nonlinear state. However, most of the traditional nonlinear solution methods are only suitable for weak nonlinear systems, but not when

the amplitude of membrane is large. Therefore, the improved multi-scale method is used to study the vibration of membrane.

2.1. Governing Equation of Vibration and Boundary Conditions

Let the length and width of the four-sided fixed membrane roof be a and b respectively; The pretension along the length direction is N_{0x} , and the pretension along the width direction is N_{0y} ; The wind blows parallel to the membrane surface, as shown in **Figure 1**. Single-mode divergent instability characterized by large vibration will occur in the state of relaxation or insufficient pre-tension of roof membrane [2]. According to the test results carried out by Usenatsu, Kimoto *et al.* [11], it is found that the film does not tear when the single-mode divergent instability occurs, but only the vibration displacement amplitude jumps. Therefore, this paper assumes that the film is still in the linear elastic stage when the divergent instability occurs.

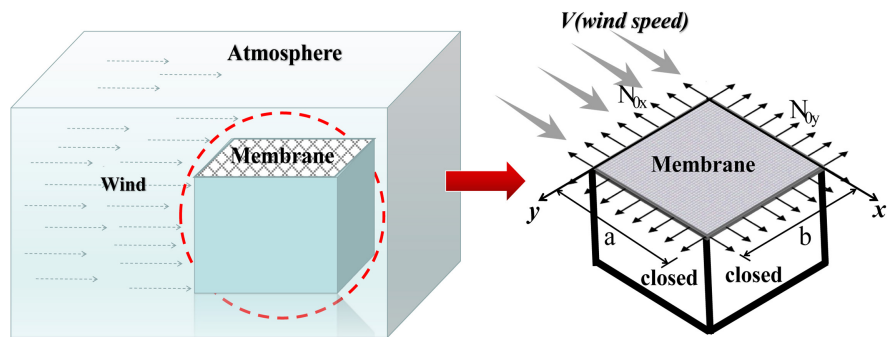


Figure 1. The membrane roof on closed structure.

When the roof membrane vibrates, the generalized external load includes wind load acting on the membrane surface, structural damping force and inertia force [2] [3]. In the process of membrane vibration, ignoring the influence of shear stress [12], the dynamic governing equations of roof membrane are as follows:

$$\begin{cases} \left(N_{0y} + h \frac{\partial^2 \varphi}{\partial x^2} \right) k_y + \left(N_{0x} + h \frac{\partial^2 \varphi}{\partial y^2} \right) k_x + p - 2\rho c \frac{\partial w}{\partial t} - \rho \frac{\partial^2 w}{\partial t^2} = 0 \\ \frac{1}{E_1} \frac{\partial^4 \varphi}{\partial y^4} + \frac{1}{E_2} \frac{\partial^4 \varphi}{\partial x^4} = \left(\frac{\partial^2 w}{\partial x \partial y} \right)^2 - \frac{\partial^2 w}{\partial x^2} \frac{\partial^2 w}{\partial y^2} - k_{0x} \frac{\partial^2 w}{\partial y^2} - k_{0y} \frac{\partial^2 w}{\partial x^2} \end{cases} \quad (1)$$

where h is the thickness of the film; E_1 and E_2 represent Young's modulus of elasticity in the x -direction and y -direction, respectively; w represents the normal vibration displacement of the membrane material; ρ is the surface density of the film material; c represents the damping coefficient of membrane material; $\varphi = \varphi(x, y, t)$ denotes the stress function.

The membrane roof is fixed on four sides, so the boundary conditions are:

$$\begin{cases} w(0, y, t) = 0 \\ w(a, y, t) = 0 \end{cases}, \begin{cases} w(x, 0, t) = 0 \\ w(x, b, t) = 0 \end{cases} \quad (2)$$

2.2. Solution of Vibration Governing Equation

Since the initial surface function of the membrane roof is $z_0(x, y) = 0$, the surface equation of the roof under wind load is

$$z(x, y, t) = w(x, y, t) \tag{3}$$

The initial curvature of the roof membrane and the curvature during vibration are

$$\begin{cases} k_{0x} = \frac{\partial^2 z_0}{\partial x^2} = 0, & k_x = \frac{\partial^2 z}{\partial x^2} = \frac{\partial^2 w}{\partial x^2} \\ k_{0y} = \frac{\partial^2 z_0}{\partial y^2} = 0, & k_y = \frac{\partial^2 z}{\partial y^2} = \frac{\partial^2 w}{\partial y^2} \end{cases} \tag{4}$$

Let the solution of the governing equation be [12]

$$w(x, y, t) = T(t) \sin \frac{m\pi x}{a} \sin \frac{n\pi y}{b} \tag{5}$$

In reference [2], the partial differential equation of wind-induced vibration of membrane roof is obtained as follows:

$$\begin{aligned} & \left(\rho W + \frac{\rho_0}{\pi} \gamma_1 \right) \frac{d^2 T(t)}{dt^2} + \left[\frac{\rho_0 V}{2\pi} (\gamma_2 - \gamma_4) + 2\rho c W \right] \frac{dT(t)}{dt} \\ & - \left(N_{0x} \frac{\partial^2 W}{\partial x^2} + N_{0y} \frac{\partial^2 W}{\partial y^2} + \frac{\rho_0 V^2}{2\pi} \gamma_3 \right) T(t) \\ & - h \left(\frac{\partial^2 \Phi}{\partial y^2} \frac{\partial^2 W}{\partial x^2} + \frac{\partial^2 \Phi}{\partial x^2} \frac{\partial^2 W}{\partial y^2} \right) T^3(t) = 0 \end{aligned} \tag{6}$$

where,

$$\begin{aligned} \gamma_1 &= \iint_{Ra} \frac{1}{r} (W)_{x=\xi, y=\eta} d\xi d\eta = \iint_{Ra} \frac{1}{r} \sin \frac{m\pi\xi}{a} \sin \frac{n\pi\eta}{b} d\xi d\eta \\ \gamma_2 &= \iint_{Ra} \frac{1}{r} \left(\frac{\partial W}{\partial x} \right)_{x=\xi, y=\eta} d\xi d\eta = \frac{m\pi}{a} \iint_{Ra} \frac{1}{r} \cos \frac{m\pi\xi}{a} \sin \frac{n\pi\eta}{b} d\xi d\eta \\ \gamma_3 &= \iint_{Ra} \frac{1}{r^3} \left(\frac{\partial W}{\partial x} \right)_{x=\xi, y=\eta} (x - \xi) d\xi d\eta = \frac{m\pi}{a} \iint_{Ra} \frac{1}{r^3} (x - \xi) \cos \frac{m\pi\xi}{a} \sin \frac{n\pi\eta}{b} d\xi d\eta \\ \gamma_4 &= \iint_{Ra} \frac{1}{r^3} (W)_{x=\xi, y=\eta} (x - \xi) d\xi d\eta = \iint_{Ra} \frac{1}{r^3} (x - \xi) \sin \frac{m\pi\xi}{a} \sin \frac{n\pi\eta}{b} d\xi d\eta \end{aligned}$$

Equation (6) is integrated using the Bubnov-Galerkin method, yields,

$$\begin{aligned} & \iint_S \left\{ \left(\rho W + \frac{\rho_0}{\pi} \gamma_1 \right) \frac{d^2 T(t)}{dt^2} + \left[\frac{\rho_0 V}{2\pi} (\gamma_2 - \gamma_4) + 2\rho c W \right] \frac{dT(t)}{dt} \right. \\ & - \left(N_{0x} \frac{\partial^2 W}{\partial x^2} + N_{0y} \frac{\partial^2 W}{\partial y^2} + \frac{\rho_0 V^2}{2\pi} \gamma_3 \right) T(t) \\ & \left. - h \left(\frac{\partial^2 \Phi}{\partial y^2} \frac{\partial^2 W}{\partial x^2} + \frac{\partial^2 \Phi}{\partial x^2} \frac{\partial^2 W}{\partial y^2} \right) T^3(t) \right\} W(x, y) dx dy = 0 \end{aligned} \tag{7}$$

The integration region in Equation (7) is $S \in \{0 \leq x \leq a, 0 \leq y \leq b\}$.

Simplifying Equation (7), yields,

$$\begin{aligned} & \left(\frac{\rho\pi ab + 4\rho_0\alpha_1}{4\pi} \right) \frac{d^2T(t)}{dt^2} + \left(\frac{\rho_0\pi mV\alpha_2 - a\rho_0V\alpha_4 + \rho\pi ca^2b}{2\pi a} \right) \frac{dT(t)}{dt} \\ & + \left(\frac{m^2\pi^2b^2N_{0x} + n^2\pi^2a^2N_{0y} - 2\rho_0mV^2b\alpha_3}{4ab} \right) T(t) \\ & + \frac{h\pi^4(E_2a^4n^4 + E_1b^4m^4)}{64a^3b^3m^2} T^3(t) = 0 \end{aligned} \tag{8}$$

where

$$\begin{aligned} \alpha_1 &= \iint_S \left(\iint_{Ra} \frac{1}{r} \sin \frac{m\pi\xi}{a} \sin \frac{n\pi\eta}{b} d\xi d\eta \right) \sin \frac{m\pi x}{a} \sin \frac{n\pi y}{b} dx dy \\ \alpha_2 &= \iint_S \left(\iint_{Ra} \frac{1}{r} \cos \frac{m\pi\xi}{a} \sin \frac{n\pi\eta}{b} d\xi d\eta \right) \sin \frac{m\pi x}{a} \sin \frac{n\pi y}{b} dx dy \\ \alpha_3 &= \iint_S \left(\iint_{Ra} \frac{1}{r^3} (x - \xi) \cos \frac{m\pi\xi}{a} \sin \frac{n\pi\eta}{b} d\xi d\eta \right) \sin \frac{m\pi x}{a} \sin \frac{n\pi y}{b} dx dy \\ \alpha_4 &= \iint_S \left[\iint_{Ra} \frac{1}{r^3} (x - \xi) \sin \frac{m\pi\xi}{a} \sin \frac{n\pi\eta}{b} d\xi d\eta \right] \sin \frac{m\pi x}{a} \sin \frac{n\pi y}{b} dx dy \end{aligned}$$

In Equation (8), $\frac{\rho\pi ab + 4\rho_0\alpha_1}{4\pi} \neq 0$, Let $x = x(t) = T(t)$, according to the calculation principle of improved multi-scale method [13], take the perturbation parameters as $\varepsilon = \frac{h\pi^5(E_2a^4n^4 + E_1b^4m^4)}{16a^3b^3m^2(\rho\pi ab + 4\rho_0\alpha_1)}$, then, Equation (8) can be simplified as:

$$\ddot{x} + \omega_0^2 x + \varepsilon(\mu\dot{x} + x^3) = 0 \tag{9}$$

where,

$$\begin{aligned} \omega_0^2 &= \frac{\pi(m^2\pi^2b^2N_{0x} + n^2\pi^2a^2N_{0y} - 2\rho_0mV^2b\alpha_3)}{ab(\rho\pi ab + 4\rho_0\alpha_1)} \\ u &= \frac{2(\rho_0\pi mV\alpha_2 - a\rho_0V\alpha_4 + \rho\pi ca^2b)}{a\varepsilon(\rho\pi ab + 4\rho_0\alpha_1)} \end{aligned}$$

Let ω be the vibration frequency of the roof membrane, and expand ω^2 near ω_0^2 into a power series of ε , that is,

$$\omega^2 = \omega_0^2 + \varepsilon\omega_1 + \varepsilon^2\omega_2 + \dots \tag{10}$$

Letting,

$$\alpha = \frac{\varepsilon\omega_1}{\omega_0^2 + \varepsilon\omega_1} \tag{11}$$

Then,

$$\varepsilon = \frac{\omega_0^2\alpha}{\omega_1(1 - \alpha)} \tag{12}$$

$$\omega_0^2 + \varepsilon\omega_1 = \frac{\omega_0^2}{1-\alpha}$$

Expand ω^2 into a power series of ε [14],

$$\begin{aligned} \omega^2 &= \omega_0^2 + \varepsilon\omega_1 \left[1 + \frac{1}{\omega_0^2 + \varepsilon\omega_1} (\varepsilon^2\omega_2 + \varepsilon^3\omega_3 + \dots) \right] \\ &= \frac{\omega_0^2}{1-\alpha} (1 + \delta_2\alpha^2 + \delta_3\alpha^3 + \dots) \end{aligned} \tag{13}$$

$$\omega = \omega_0 \left[1 + \frac{1}{2}\alpha + \left(\frac{3}{8} + \frac{\delta^2}{2} \right) \alpha^2 + \dots \right] \tag{14}$$

The solution of Equation (9) can be assumed to be

$$x(t, \alpha) = x_0(T_0, T_1) + \alpha x_1(T_0, T_1) + \alpha^2 x_2(T_0, T_1) + \dots \tag{15}$$

where $T_0 = t, T_1 = \alpha t$.

The differential operators can be obtained as follows:

$$\begin{aligned} \frac{d}{dt} &= D_0 + \alpha D_1 + \alpha^2 D_2 + \dots, \\ \frac{d^2}{dt^2} &= D_0^2 + 2\alpha D_0 D_1 + \alpha^2 (D_1^2 + 2D_0 D_2) + \dots \end{aligned} \tag{16}$$

By substituting Equations (11)-(13) and (16) into Equation (9) and collating, we can obtain:

$$\begin{aligned} &(1-\alpha) \left[D_0^2 + 2\alpha D_0 D_1 + \alpha^2 (D_1^2 + 2D_0 D_2) \right] (x_0 + \alpha x_1 + \alpha^2 x_2 + \dots) \\ &+ (1-\alpha) \omega_0^2 (x_0 + \alpha x_1 + \alpha^2 x_2 + \dots) + \frac{\alpha \omega_0^2}{\omega_1^2} \left[(x_0 + \alpha x_1 + \alpha^2 x_2 + \dots)^3 \right. \\ &\left. + (D_0 + \alpha D_1 + \alpha^2 D_2) \cdot (x_0 + \alpha x_1 + \alpha^2 x_2 + \dots) \right] = 0 \end{aligned} \tag{17}$$

Expand Equation (17), let the coefficients of each power of α in the equation be zero, yields,

$$\begin{aligned} \alpha^0 \quad &D_0^2 x_0 + \omega_0^2 x_0 = 0 \\ \alpha^1 \quad &D_0^2 x_1 + \omega_0^2 x_1 + 2D_0 D_1 x_0 + \frac{\omega_0^2}{\omega_1} (D_0 x_0 + x_0^3) = 0 \\ \alpha^2 \quad &D_0^2 x_2 + x_2 + 2D_0 D_1 x_1 + (D_1^2 + 2D_0 D_2) x_0 + \frac{\omega_0^2}{\omega_1} 3x_0^2 x_1 = 0 \end{aligned} \tag{18}$$

The solution of the first equation in the system of Equation (18) can be

$$x_0 = A(T_1) e^{i\omega_0 T_0} + \bar{A}(T_1) e^{-i\omega_0 T_0} \tag{19}$$

By substituting Equation (19) into α^1 , yields:

$$D_0^2 x_1 + \omega_0^2 x_1 + \left(2i\omega_0 D_1 A + 3 \frac{\omega_0^2}{\omega_1} A^2 \bar{A} + i\mu \frac{\omega_0^3}{\omega_1} A \right) e^{i\omega_0 T_0} + \frac{1}{\omega_1} A^3 e^{3i\omega_0 T_0} + cc = 0 \tag{20}$$

Where cc is a conjugate complex number, let:

$$2D_1 A + 3 \frac{\omega_0}{\omega_1} A^2 \bar{A} + i\mu \frac{\omega_0^3}{\omega_1} A = 0 \tag{21}$$

Solving Equations (21), yields

$$x_1 = \frac{1}{8\omega_1} \left(A^3 e^{3iT_0} + \bar{A}^3 e^{-3iT_0} \right) \quad (22)$$

Let $A = \frac{1}{2} f e^{i\phi}$, then substitute it into Equation (22) and separate the imaginary and real parts,

$$\frac{df}{dT_1} = -\frac{1}{2} \mu \frac{\omega_0^2}{\omega_1} f, \quad f \frac{d\phi}{dT_1} = -\frac{3\omega_0}{8\omega_1} f^3 \quad (23)$$

substitute $A = \frac{1}{2} f e^{i\phi}$ into Equation (19), yields:

$$x_0 = f \cos(\omega_0 T_0 + \phi) = f \cos(\omega t + \phi_0) \quad (24)$$

It can be obtained from Equations (24) and (14) that under the first-order approximation condition

$$\frac{d\phi}{dT_1} = \frac{\omega_0}{2} \quad (25)$$

Combining Equations (23) and (25), yields:

$$\omega_1 = \frac{3}{4} f^2 \quad (26)$$

By substituting Equation (26) into Equation (23) and omitting the higher-order terms, yields:

$$\omega = \sqrt{\omega_0^2 + \frac{3}{4} \varepsilon f^2} \quad (27)$$

The existing research results show that when the membrane roof reaches the critical state of instability, the frequency of the characteristic equation of the system approaches zero [2] [3]. *i.e.*:

$$\omega_0^2 + \frac{3}{4} \varepsilon f^2 = 0 \quad (28)$$

where f is the vibration amplitude of the membrane material.

$$\omega_0^2 = \frac{\pi(m^2 \pi^2 b^2 N_{0x} + n^2 \pi^2 a^2 N_{0y} - 2\rho_0 m V^2 b \alpha_3)}{ab(\rho \pi ab + 4\rho_0 \alpha_1)}$$

From Equation (28), the critical wind speed when the roof membrane material is instable can be obtained as follows:

$$V_{cr} = \sqrt{\frac{4\pi(m^2 \pi^2 b^2 N_{0x} + n^2 \pi^2 a^2 N_{0y}) + 3\varepsilon f^2 (\rho \pi a^2 b^2 + 4\rho_0 ab \alpha_1)}{8\pi b \rho_0 m \alpha_3}} \quad (29)$$

where f is the vibration amplitude, that is, the vibration amplitude corresponding to the critical wind speed of instability. It shows that the critical wind speed is related to the vibration amplitude. Because the geometric nonlinear influence of membrane is considered, the stiffness of membrane will change with the change of amplitude in the vibration process, which will affect the stability of the structure

to a certain extent, which is consistent with the existing research results. When $f \rightarrow 0$, the critical wind speed calculated according to the small deflection theory can be obtained.

3. Minimum Pre-Tension of Membrane Roof

The principle of determining the safety pre-tension of the membrane roof under a specific site is that under the local design maximum wind speed, the membrane roof will not be instable and damaged, that is, the local design maximum wind speed is less than or equal to the critical wind speed of instability, that is:

$$V \leq V_{cr} \tag{30}$$

Substituting Equation (29) into Equation (30), yields:

$$V \leq \sqrt{\frac{4\pi(m^2\pi^2b^2N_{0x} + n^2\pi^2a^2N_{0y}) + 3\epsilon f^2(\rho\pi a^2b^2 + 4\rho_0ab\alpha_1)}{8\pi b\rho_0m\alpha_3}} \tag{31}$$

where, V is the local design wind speed.

$$V \leq \left(\sqrt{\frac{4\pi(m^2\pi^2b^2N_{0x} + n^2\pi^2a^2N_{0y}) + 3\epsilon f^2(\rho\pi a^2b^2 + 4\rho_0ab\alpha_1)}{8\pi b\rho_0m\alpha_3}} \right)_{\min} \tag{32}$$

Simplify Equation (32), yields:

$$N_{0x} + \frac{a^2}{b^2}N_{0y} \geq \frac{2\rho_0\alpha_3}{b\pi}V^2 \tag{33}$$

Equation (33) is the formula for determining the safety pretension limit of membrane roof to prevent instability. When the span ratio of roof membrane is determined, the safe pretension value can be obtained.

Let $E_1 = 900 \text{ MPa}$, $E_2 = 1400 \text{ MPa}$, $\rho_0 = 1.226 \text{ kg/m}^3$, $h = 0.001 \text{ m}$, $N_{0x} = N_{0y}$.

The results of safety pretension limits of membrane roofs in a certain area are shown in **Table 1**.

Table 1. Safety pretension limit of membrane roof.

Design Return Period/Years	$V_{cr}/(\text{m/s})$	Roof length/(m)	Roof width/(m)	Safety pretension limit/(kN/m)
10	20	5	10	1.223
		10	10	1.434
		20	10	1.245
50	25.3	5	10	1.957
		10	10	2.295
		20	10	1.993
100	26.83	5	10	2.200
		10	10	2.581
		20	10	2.241

4. Conclusions

In this paper, the traditional multi-scale method is improved to solve the critical state of instability of membrane roof. In order to avoid the instability of the roof during the design return period, the critical wind speed of instability should not be less than the local design wind speed, so that the calculation formula of the minimum pretension of the roof film to prevent instability in different return periods of a specific wind field is obtained, and the following conclusions are obtained.

1) The critical wind speed of nonlinear wind-induced instability of membrane roof is related to membrane pretension, geometric size, density and vibration amplitude.

2) The safety pretension limit of membrane roof to prevent instability is related to the design wind speed and membrane geometry. This paper supplements the specific requirements on the value of pretension in the technical specification of membrane structure (CECS158: 2015) [15], and provides a theoretical basis for engineering designers to reasonably design membrane structure.

Conflicts of Interest

The authors declare no conflicts of interest regarding the publication of this paper.

References

- [1] Shen, S.Z. and Wu, Y. (2006) Research Progress on Fluid-Solid Interaction Effect of Wind-Induced Vibration Response of Membrane Structure. *Journal of Architecture and Civil Engineering*, **23**, 1-9.
- [2] Zheng, Z., Xu, Y., Liu, C., He, X. and Song, W. (2011) Nonlinear Aerodynamic Stability Analysis of Orthotropic Membrane Structures with Large Amplitude. *Structural Engineering and Mechanics*, **37**, 401-413. <https://doi.org/10.12989/sem.2011.37.4.401>
- [3] Xu, Y., Zheng, Z., Liu, C., Song, W. and Long, J. (2011) Aerodynamic Stability Analysis of Geometrically Nonlinear Orthotropic Membrane Structure with Hyperbolic Paraboloid. *Journal of Engineering Mechanics*, **137**, 759-768. [https://doi.org/10.1061/\(asce\)em.1943-7889.0000278](https://doi.org/10.1061/(asce)em.1943-7889.0000278)
- [4] Chen, Z.Q. (2015) Aeroelastic Instability Mechanism of Tensioned Membrane Structures. Harbin University of Technology.
- [5] Liu, C., Deng, X. and Zheng, Z. (2017) Nonlinear Wind-Induced Aerodynamic Stability of Orthotropic Saddle Membrane Structures. *Journal of Wind Engineering and Industrial Aerodynamics*, **164**, 119-127. <https://doi.org/10.1016/j.jweia.2017.02.006>
- [6] Li, Q.X. and Sun, B.N. (2006) Wind-Induced Aerodynamic Instability Analysis for Closed Membrane Roofs. *Journal of Vibration Engineering*, **19**, 346-353.
- [7] Wu, Y., Sun, X. and Shen, S. (2008) Computation of Wind-Structure Interaction on Tension Structures. *Journal of Wind Engineering and Industrial Aerodynamics*, **96**, 2019-2032. <https://doi.org/10.1016/j.jweia.2008.02.043>
- [8] Zheng, Z.-L., *et al.* (2009) Free Vibration Analysis of Rectangular Orthotropic Membranes in Large Deflection. *Mathematical Problems in Engineering*, **2009**, Article ID: 634362. <https://doi.org/10.1155/2009/634362>

-
- [9] Li, Q.X. and Sun, B.N. (2006) Parametric Resonance Analysis of Closed Membrane Roofs. *Journal of Aerodynamics*, **24**, 55-61.
- [10] Yang, Q.S. and Liu, R.X. (2006) On Aerodynamic Stability of Membrane Structures. *Engineering Mechanics*, **23**, 18-24, 29.
- [11] Stanford, B., Sytsma, M., Albertani, R., Viieru, D., Shyy, W. and Ifju, P. (2007) Static Aeroelastic Model Validation of Membrane Micro Air Vehicle Wings. *AIAA Journal*, **45**, 2828-2837. <https://doi.org/10.2514/1.30003>
- [12] Zheng, Z., Song, W., Liu, C., He, X., Sun, J. and Xu, Y. (2012) Study on Dynamic Response of Rectangular Orthotropic Membranes under Impact Loading. *Journal of Adhesion Science and Technology*, **26**, 1467-1479. <https://doi.org/10.1163/156856111x618335>
- [13] Li, Y.M., Song, W.J. and Wang, X.W. (2019) Analytical Solutions to Strongly Non-linear Vibration of a Clamped Membrane Structure. *Journal of Vibration and Shock*, **38**, 144-148, 177.
- [14] Chen, S.H. (2009) Quantitative Analysis Method for Strong Nonlinear Vibration Systems. Science Press.
- [15] China Association for Standardization of Engineering Construction (2015) Technical Regulations for Membrane Structure: CECS158: 2015. China Planning Publishing House.